



Carbon isotope composition of basalts from Loihi Seamount: Primordial or recycled carbon in the Hawaiian mantle plume?

David W. Graham ^{a,*}, Peter J. Michael ^b, Thi B. Truong ^a

^a College of Earth, Ocean, and Atmospheric Sciences, Oregon State University, Corvallis, OR 97331, United States of America
^b Department of Geosciences, The University of Tulsa, 800 S. Tucker Drive, Tulsa, OK 74104, United States of America

ARTICLE INFO

Article history:

Received 6 March 2023

Received in revised form 17 May 2023

Accepted 27 May 2023

Available online xxxx

Editor: F. Moynier

Dataset link: <https://doi.org/10.26022/IEDA/112511>

Keywords:

Loihi Seamount

Kama'ehuakanaloa

carbon isotopes

helium isotopes

mantle plume

ABSTRACT

We analyzed the carbon isotope composition of vesicle CO_2 , plus He isotopes and He and CO_2 concentrations in the vesicle (vapor) and glass (melt) phases of 37 submarine basalts from the summit, north and south rifts, and east flank of Loihi Seamount. Tholeiites and transitional basalts lie in a narrow range of vesicle $\delta^{13}\text{C} = -4.6$ to $-0.9\text{\textperthousand}$, while alkali basalts range from -7.2 to $-2.1\text{\textperthousand}$. Calculated total (vesicle+glass) $\delta^{13}\text{C}$ for the majority of the basalts ranges from -6 to $-2\text{\textperthousand}$ assuming the vapor-melt fractionation factor Δ ($= \delta_{\text{vapor}} - \delta_{\text{melt}}$) is $+2$ to $+4\text{\textperthousand}$ as measured in basaltic systems. This relatively narrow range of $\delta^{13}\text{C}$ resembles mantle source values deduced from gas-rich mid-ocean ridge basalts and basalts from Iceland, and for Kilauea volcano deduced from its fumarole gas. However, this similarity presents a conundrum because Loihi basalts have degassed $>97\%$ of their initial CO_2 as deduced from CO_2 - Ba systematics and crystal fractionation modeling.

Loihi parental magma ($\text{MgO}=18$ wt.%) had initial CO_2 concentrations of 0.6 to 1.9 wt.%. Most tholeiitic and transitional basalts appear to have followed a quasi closed-system degassing history. Correcting for this degassing indicates the median $\delta^{13}\text{C}$ for Loihi undegassed parental magmas is $-1.5\text{\textperthousand}$ and the $\delta^{13}\text{C}$ range is -4 to $+1\text{\textperthousand}$. Estimates of this $\delta^{13}\text{C}$ range are only weakly dependent on the choice of Δ and initial $[\text{CO}_2]$ in closed-system degassing scenarios. The Loihi mantle plume source is therefore characterized by $\delta^{13}\text{C}$ values that are higher than the range of -6 to $-4\text{\textperthousand}$ prevalent in mantle-derived basalts and many diamonds. This could be due to primordial carbon isotope heterogeneity in Earth's mantle, exchange of carbon at the core-mantle boundary between ultra-low velocity zone silicates and the metallic liquid outer core, or to the presence of a small fraction ($<1\%$ by mass) of surficial carbonate that was tectonically recycled to the Hawaiian plume source region. Currently, an origin from recycled carbonate has the most supporting evidence.

© 2023 Elsevier B.V. All rights reserved.

1. Introduction

When lithosphere is subducted to the deep mantle from Earth's surface, it can mix with pools of ancient (>4.45 Ga) material that are thought to comprise parts of either the large low shear velocity provinces (LLSVPs) or ultra-low velocity zones (ULVZs) at the core-mantle boundary (McNamara, 2019). Some of the geochemical and isotopic variations in ocean island lavas result from such admixtures of recycled slab components, including oceanic crust and sediments (White, 1985), with ancient (primordial?) mantle in this deep region. This mixing can lead to ocean island lavas having variable helium isotope ratios. High ${}^3\text{He}/{}^4\text{He}$ ratios indicate the presence of relatively undegassed mantle in the plume

source of ocean island hotspots such as Hawaii and Iceland, while lower ${}^3\text{He}/{}^4\text{He}$ ratios indicate the presence of recycled material (Kurz et al., 1982). This dichotomy involving both ancient mantle and younger recycled materials in the petrogenesis of ocean islands is now a central tenet of geodynamic models (Li et al., 2014; Williams et al., 2015; Gölcher et al., 2021). High ${}^3\text{He}/{}^4\text{He}$ ratios have also been linked with anomalously slow seismic velocities near the core-mantle boundary (Williams et al., 2019), and with ${}^{182}\text{W}$ anomalies produced by radioactive decay of extinct ${}^{182}\text{Hf}$ (Mundl-Petermeier et al., 2020). These observations further suggest there may be some influence of Earth's outer core on the behavior and composition of mantle plumes.

One important challenge in mantle geodynamics has been to determine the source of carbon at ocean island hotspots, such as Hawaii, that originate from deep mantle plumes (Anderson and Poland, 2017; Tucker et al., 2019). To quantify the proportion of carbon that may be recycled vs. primordial, precise CO_2 abundance

* Corresponding author.

E-mail address: david.graham@oregonstate.edu (D.W. Graham).

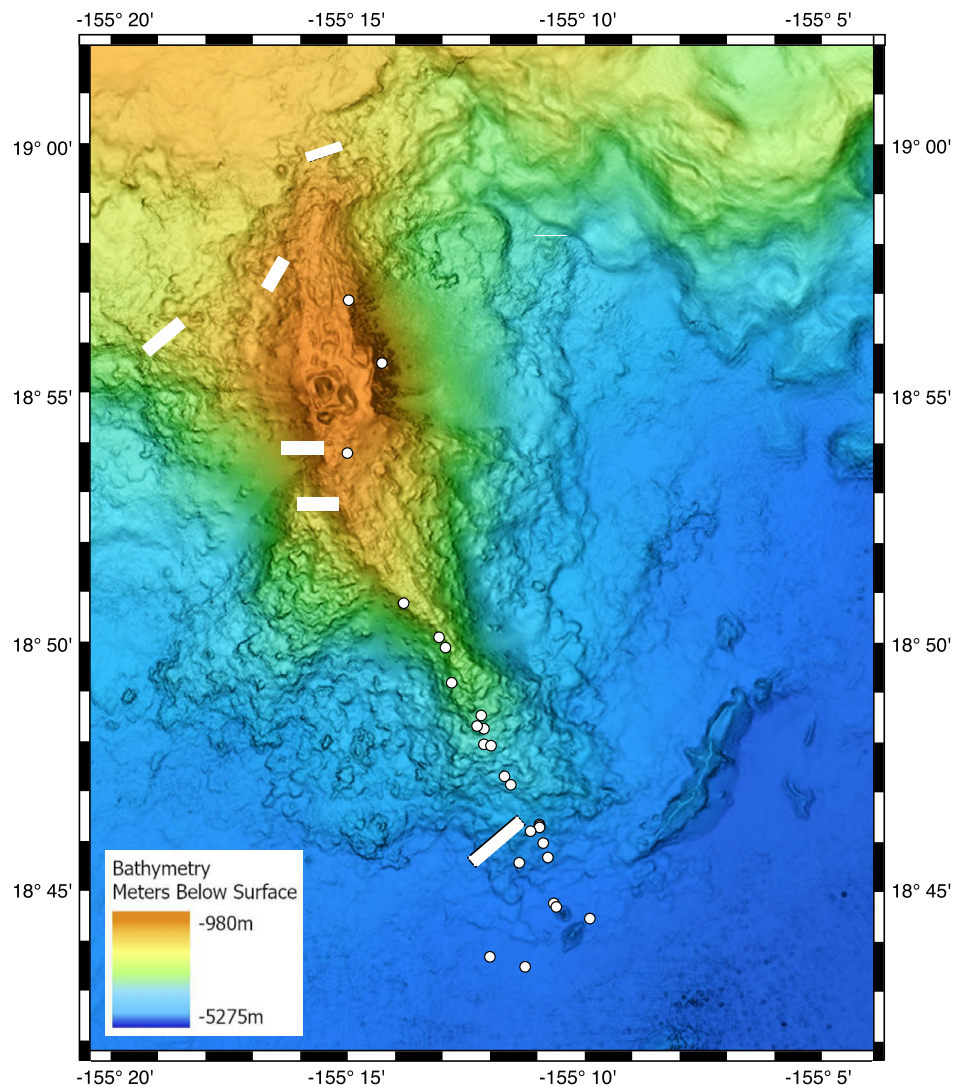


Fig. 1. Sample location map. White bars show dredge tracks and white circles show locations of submersible samples.

and carbon isotope data need to be obtained for the same samples analyzed for helium isotopes. These data must then be corrected for possible fractionation during volatile loss - of CO_2 from He and of ^{13}C from ^{12}C - because virtually all basalts become CO_2 -oversaturated and degas variable amounts of CO_2 during ascent and eruption, and so they do not preserve their original magmatic CO_2 contents, CO_2/He ratios, or $\delta^{13}\text{C}$. The current study aims to address the origin of primordial vs. recycled carbon in mantle plumes, by characterizing the C isotope compositions of high $^3\text{He}/^4\text{He}$ basalts erupted at Loihi Seamount (Kama'ehuakanaloa), the youngest volcano in the Hawaiian volcanic chain.

2. Methods

We analyzed 37 basalt glass samples (Fig. 1), predominantly from the deep south rift zone of Loihi Seamount ($n=26$), with additional samples from the summit ($n=5$), east flank ($n=3$) and northern rift ($n=3$). Several of the south rift samples were analyzed previously for noble gases by Valbracht et al. (1996, 1997) and Kaneoka et al. (2002), and four glass samples were analyzed by ion microprobe for dissolved CO_2 by Pietruszka et al. (2011). Our analytical procedures are described in previous studies (Graham et al., 2014; Graham and Michael, 2021). $^3\text{He}/^4\text{He}$ ratios and He concentrations were measured in both the vesicles and glass phase of each sample at OSU. During the crushing extraction of

vesicle helium, we measured the amount of vesicle CO_2 by capacitance manometry. After helium isotope analysis, the vesicle CO_2 was transferred to glass ampoules and subsequently analyzed by mass spectrometry for its C isotope composition. Dissolved CO_2 and H_2O in the glass phase were analyzed by Fourier Transform Infrared Spectrometry at UT (Michael and Graham, 2015). Major elements were determined by electron microprobe at UH (Garcia et al., 1995), and trace elements by laser ablation ICP-MS at OSU following procedures similar to those described in Michael and Graham (2015) and Graham and Michael (2021).

We distinguish basalt types using the Alkalinity Index (AI) defined by Carmichael et al. (1974) based on a sample's position in the total alkalis - silica diagram: $\text{AI} = (\text{Na}_2\text{O} + \text{K}_2\text{O}) - (0.37\text{SiO}_2 - 14.43)$. The AI yields a more consistent geochemical delineation of Loihi Seamount samples than estimates of silica saturation based on normative nepheline. Basalt types in the study are roughly evenly distributed: there are 12 tholeites ($\text{AI} < 0$), 14 transitional basalts ($0 < \text{AI} < 1$) and 11 alkali basalts ($\text{AI} > 1$).

3. Results

Results of this study are presented in the **Supplementary Information** (Table S1). Vesicle $^3\text{He}/^4\text{He}$ ranges from 20–32 R_A in our sample suite, with typical 2-sigma uncertainties of 0.2–0.4 R_A .

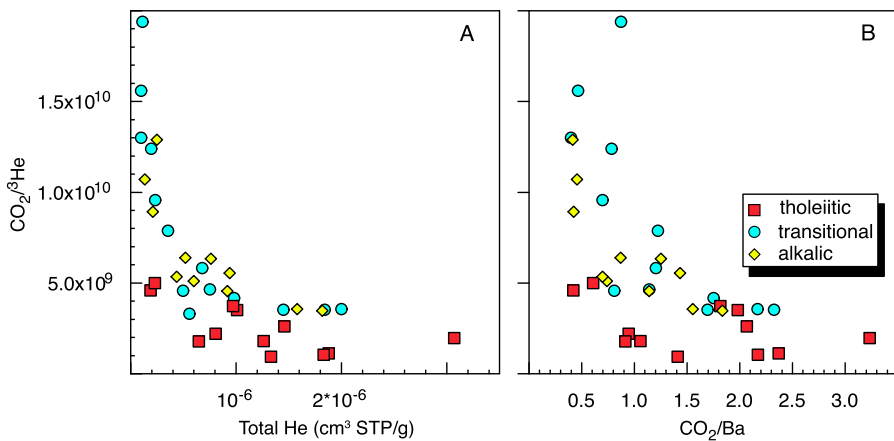


Fig. 2. A. Total $\text{CO}_2/{}^3\text{He}$ vs. total $[\text{He}]$. B. Total $\text{CO}_2/{}^3\text{He}$ vs. Total CO_2/Ba for Loihi basalts.

Tholeiites range to higher ${}^3\text{He}/{}^4\text{He}$ ratios ($26.3\text{--}31.9 \text{ R}_\text{A}$) than transitional ($22.1\text{--}29.1 \text{ R}_\text{A}$) and alkali basalts ($20.6\text{--}25.4 \text{ R}_\text{A}$), similar to earlier results for a smaller number of Loihi basalts (Kurz et al., 1983; Rison and Craig, 1983; Honda et al., 1993; Loewen et al., 2019).

A single evolved transitional basalt (MIR2337-b collected at 4795 m depth) yielded extremely different values from other samples, with vesicle ${}^3\text{He}/{}^4\text{He} = 4.5 \text{ R}_\text{A}$ and glass ${}^3\text{He}/{}^4\text{He} = 3.0 \text{ R}_\text{A}$. Similar to sample MIR2337-b, Kurz et al. (1983) and Rison and Craig (1983) reported low ratios in the vesicles of a differentiated alkali basalt (KK21-2, collected at 1092 m depth near the summit, having ${}^3\text{He}/{}^4\text{He} = 4.6 \text{ R}_\text{A}$ and 5.4 R_A , respectively. The low ${}^3\text{He}/{}^4\text{He}$ in KK21-2 was attributed to seawater or atmospheric interaction within that highly vesicular (25–35%) sample, despite the fresh appearance of the glass. MIR2337-b appears similarly fresh and glassy, but it has low vesicularity. This sample is not typical of basalts being erupted at Loihi Seamount and we have not considered it further in this study.

Total (vesicle + glass) He concentrations range from 1.3×10^{-7} to $3 \times 10^{-6} \text{ cm}^3 \text{ STP/g}$, and total CO_2 concentrations range from 62–510 ppm (0.032 to $0.26 \text{ cm}^3 \text{ STP/g}$). Average He and CO_2 concentrations are higher in tholeiites but there is overlap between the different basalt types. Total $\text{CO}_2/{}^3\text{He}$ ratios range from 9.4×10^8 – 1.9×10^{10} . The lowest ratios are found in tholeiites having the highest He concentrations, and are similar to mantle values deduced from oceanic basalts and xenoliths (Marty and Jambon, 1987; Trull et al., 1993). There is also a trend to higher $\text{CO}_2/{}^3\text{He}$ ratios as He concentrations decrease (Fig. 2a).

Ba ranges from 73–468 ppm and Nb ranges from 10–46 ppm. Ba is highest in basanites and alkali basalts (190–468 ppm) and lowest in tholeiites (73–150 ppm). CO_2/Ba and CO_2/Nb ratios (ppm/ppm) range from 0.4–3.3 and 3–23, respectively, and are far lower than typical mantle values of $\text{CO}_2/\text{Ba} = 70\text{--}140$ and $\text{CO}_2/\text{Nb} = 230\text{--}1000$ (Rosenthal et al., 2015; Michael and Graham, 2015; Le Voyer et al., 2017). The highest $\text{CO}_2/{}^3\text{He}$ ratios ($>5 \times 10^9$) are observed in basalts having the lowest CO_2/Ba and CO_2/Nb ratios ($\text{CO}_2/\text{Ba} < 1.5$; Fig. 2b).

Tholeiites and transitional basalts lie in a narrow range of vesicle $\delta^{13}\text{C} = -4.6$ to $-0.9\text{\textperthousand}$, while alkali basalts range from -7.2 to $-2.1\text{\textperthousand}$. Analytical uncertainties (2σ) are $<0.1\text{\textperthousand}$. These results are compared in Fig. 3 to another suite of high ${}^3\text{He}/{}^4\text{He}$ basalt glasses that we have analyzed, from the NW Lau Spreading Center that is influenced by the Samoan hotspot. A surprising result is the generally heavy C isotope nature of the vesicle CO_2 in Loihi basalts, where the median $\delta^{13}\text{C}$ is $-2.5\text{\textperthousand}$.

The vesicle C and He isotope compositions overlap with those measured in Loihi summit geothermal vent fluids in 1992 ($T < 30^\circ\text{C}$; $\delta^{13}\text{C} = -5.5$ to $-1.7\text{\textperthousand}$; ${}^3\text{He}/{}^4\text{He} = 21.7$ to 27.0 R_A ; Sed-

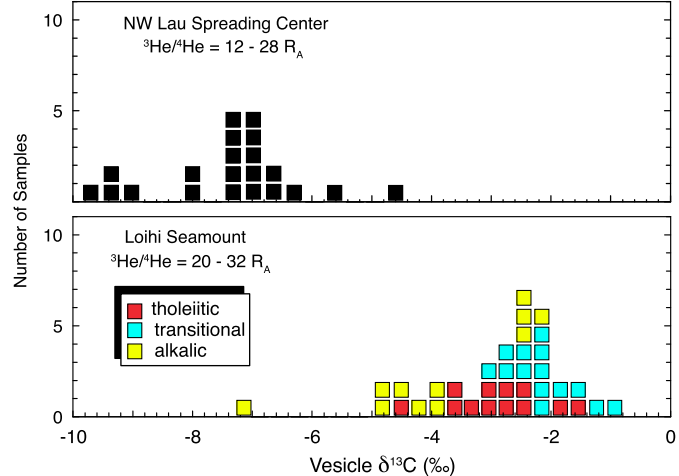


Fig. 3. A comparison of the carbon isotope results for two high ${}^3\text{He}/{}^4\text{He}$ localities; Loihi Seamount, the subject of the current study, the NW Lau Spreading Center region influenced by the Samoan mantle plume. The surprising result is the generally heavy nature of the vesicle carbon in Loihi basalts compared to typical mantle values of -4 to $-6\text{\textperthousand}$. NWLSC sample data are from IEDA (Interdisciplinary Earth Data Alliance) at <https://doi.org/10.26022/IEDA/112510>.

wick et al., 1994). This overlap supports the contention of Sedwick et al. (1994) that the anomalously low water/rock ratios (estimated from their high vent fluid $[\text{CO}_2]$ compared to low $[\text{CO}_2]$ in the lavas) imply the direct degassing of a magma body into the Loihi hydrothermal system, rather than gas stripping from the basaltic crust during fluid flow.

Our sample suite also includes five basalt glasses (samples with KK prefix) that were originally analyzed by Exley et al. (1986) for C isotopes using stepwise heating. Unfortunately, the low temperature steps in that study were dominated by surficial contamination and showed $\delta^{13}\text{C}$ as low as $-25\text{\textperthousand}$. Exley et al. (1986) suggested that vesicle CO_2 was released by the intermediate temperature steps (600–1000 °C) that had $\delta^{13}\text{C}$ between -8.3 and $-2.5\text{\textperthousand}$, with a mean value near $-6\text{\textperthousand}$. However, it seems that tailing of the low temperature contamination into those intermediate temperature steps could not be eliminated. As a result, the generally heavy character of vesicle $\delta^{13}\text{C}$ in Loihi basalts (Fig. 3) was not recognized in that study. Craig (1987) also pointed out that the analyses of Exley et al. (1986) show a correlation between the carbon released as low temperature and high temperature components, further calling into question the interpretation of magmatic values using that data. The $\delta^{13}\text{C}$ values of vesicle CO_2 in the five KK samples measured in this study lie between -4.7 and $-1.5\text{\textperthousand}$. The $\delta^{13}\text{C}$ of the dissolved CO_2 in the glass of the same five samples, determined

in the high temperature steps by Exley et al. (1986), ranged from -8.4 to $-2.8\text{\textperthousand}$, and should be considered as an accurate value for the dissolved $\delta^{13}\text{C}$.

4. Discussion

4.1. Vapor-melt fractionation and degassing effects for $\text{CO}_2/{}^3\text{He}$ and $\delta^{13}\text{C}$ in Loihi basalts

4.1.1. Kinetic effects

It is apparent that the CO_2/He ratio in many of the basalts has been strongly fractionated during degassing. The lowest $\text{CO}_2/{}^3\text{He}$ ratios of $\sim 1 \times 10^9$ are found in tholeiites having the highest He concentrations, and there is a trend to higher $\text{CO}_2/{}^3\text{He}$ ratios as He concentrations decrease (Fig. 2a). Higher $\text{CO}_2/{}^3\text{He}$ ratios are also observed in basalts having the lowest CO_2/Ba and CO_2/Nb ratios (Fig. 2b). This is evidence for extensive CO_2 degassing prior to and during eruption. In general, Loihi basalts are variably degassed and there is no simple trend between He or CO_2 concentrations and water depth (overlying pressure of eruption) or Mg# (degree of crystallization).

The factor of ten increase in $\text{CO}_2/{}^3\text{He}$ with decreasing [He] and CO_2/Ba ratio (Fig. 2) indicates that He loss is proportionally greater than CO_2 loss during magmatic evolution. This results from the diffusion rate of dissolved helium into bubbles being 1 to 3 orders of magnitude faster than for dissolved CO_3^{2-} (Tucker et al., 2018). As a consequence, vesicle CO_2/He ratios are low compared to solubility equilibrium with the volatiles in the glass. Details are discussed further in the **Supplementary Information**. The elevated total (vesicles+glass) $\text{CO}_2/{}^3\text{He}$ ratios in many Loihi basalts (especially transitional and alkali basalts having $\text{CO}_2/\text{Ba} \leq \sim 1.5$ in Fig. 2) result from significant CO_2/He fractionation associated with prior bubble loss, and so the measured $\text{CO}_2/{}^3\text{He}$ should not be taken as a reliable indicator of the mantle source. Although the lowest $\text{CO}_2/{}^3\text{He}$ ratios of $\sim 1 \times 10^9$ in the least degassed Loihi basalts may be representative of the mantle source, even these lavas have lost $>97\%$ of their original CO_2 inventory (see below), suggesting that the true $\text{CO}_2/{}^3\text{He}$ ratio of the source region might be lower.

In contrast to the $\text{CO}_2/{}^3\text{He}$ variations, significant kinetic fractionation is not apparent in the $\delta^{13}\text{C}$ variations, presumably because the difference in diffusion rate of ${}^{13}\text{CO}_3^{2-}/{}^{12}\text{CO}_3^{2-}$ in basaltic magma is far less than it is for $\text{CO}_3^{2-}/{}^3\text{He}$. Fig. 4 shows $\delta^{13}\text{C}$ of dissolved CO_2 (using step-heating data from Exley et al., 1986) compared to vesicle $\delta^{13}\text{C}$ obtained by crushing the same basalt glass samples in this study. Few paired $\delta^{13}\text{C}$ data have been obtained in this way for ocean hotspots because only a couple labs in the world have the capability to avoid significant carbon contamination during the heating extraction of C from the glass. The experimentally determined equilibrium fractionation between vapor and melt ($\Delta_{\text{vapor-melt}} = \delta^{13}\text{C}_{\text{vapor}} - \delta^{13}\text{C}_{\text{melt}}$) ranges between $+2$ and $+4\text{\textperthousand}$, with the gas phase enriched in the heavy isotope (Javoy et al., 1978; Matthey, 1991; Matthey et al., 1990). Pure kinetic fractionation would show vapor enrichment in ${}^{12}\text{C}$, with observed $\Delta_{\text{vapor-melt}} = -8.2\text{\textperthousand}$ (Aubaud, 2022). Three of the five KK basalts have apparent $\Delta_{\text{vapor-melt}}$ values of $+2$ to $+4\text{\textperthousand}$ similar to the experimentally determined value (Fig. 4). One sample may show partial kinetic fractionation (apparent $\Delta_{\text{vapor-melt}} = -1\text{\textperthousand}$) while another has apparent $\Delta_{\text{vapor-melt}} = +6\text{\textperthousand}$. Kinetic fractionation also does not account for the $\delta^{13}\text{C}$ variations at other OIB localities (Fig. 4), which have a range of $\Delta_{\text{vapor-melt}}$ values that is similar to Loihi's range. Collectively, the Loihi basalt data are shifted to $\delta^{13}\text{C}$ values that are heavier than mid-ocean ridge basalts and hotspot basalts from Pitcairn and Society Islands (Fig. 4).

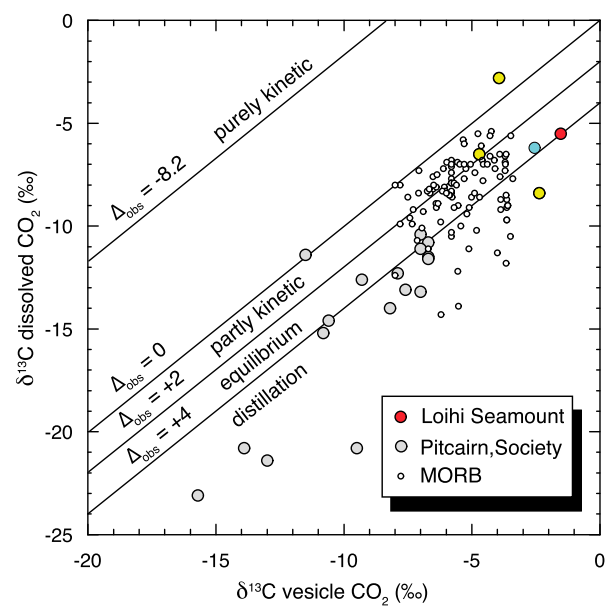


Fig. 4. Dissolved (glass) $\delta^{13}\text{C}$ compared to vapor (vesicle) $\delta^{13}\text{C}$ for submarine basalt glasses from mid-ocean ridges and ocean island hotspots, modified from Aubaud (2022). Loihi data are shown by the solid circles (red-tholeiite, blue-transitional basalt, yellow-alkali basalt). $\delta^{13}\text{C}$ of Loihi dissolved CO_2 is from the high-temperature step-heating measurements of Exley et al. (1986), and vesicle data for the same samples are from this study. The experimentally determined equilibrium fractionation between vapor and melt ranges between $+2$ and $+4\text{\textperthousand}$ (Javoy et al., 1978; Matthey, 1991; Matthey et al., 1990) and is depicted by the solid lines. Pure kinetic fractionation has vapor enrichment in ${}^{12}\text{C}$ with a vapor-melt fractionation factor of $-8.2\text{\textperthousand}$ (Aubaud, 2022).

4.1.2. $\delta^{13}\text{C}$ of total CO_2 (vesicle+glass) in Loihi basalts

In this section we estimate the range of $\delta^{13}\text{C}$ for the total CO_2 (vesicle+glass) in Loihi basalts. Because there are no measurements of $\delta^{13}\text{C}$ for the dissolved CO_2 in most of our samples, we reconstruct $\delta^{13}\text{C}$ for the dissolved CO_2 and estimate $\delta^{13}\text{C}$ of total CO_2 using specified values of $\Delta_{\text{vapor-melt}}$ ($\Delta = \delta^{13}\text{C}_{\text{vesicles}} - \delta^{13}\text{C}_{\text{glass}}$).

The bulk system (total) $\delta^{13}\text{C}$ is the sum of two products: 1) the product of vapor $\delta^{13}\text{C}$ with the fraction of CO_2 in the vapor, and 2) the product of melt $\delta^{13}\text{C}$ with the fraction of CO_2 in the melt.

$$\delta^{13}\text{C}_{\text{total}} = \delta^{13}\text{C}_{\text{v}} F_{\text{v}} + \delta^{13}\text{C}_{\text{g}} F_{\text{g}} \quad (1)$$

where F_{v} is the fraction of CO_2 in the vesicles (vapor) ($F_{\text{v}} = \left(\frac{[\text{CO}_2]_{\text{v}}}{[\text{CO}_2]_{\text{v}} + [\text{CO}_2]_{\text{g}}} \right)$), and F_{g} is the fraction of CO_2 in the glass (melt) ($F_{\text{g}} = \left(\frac{[\text{CO}_2]_{\text{g}}}{[\text{CO}_2]_{\text{v}} + [\text{CO}_2]_{\text{g}}} \right)$). This ultimately leads to (see the **Supplementary Information** for details)

$$\delta^{13}\text{C}_{\text{total}} = \delta^{13}\text{C}_{\text{v}} - \Delta_{\text{vapor-melt}} \left(\frac{[\text{CO}_2]_{\text{g}}}{[\text{CO}_2]_{\text{v}} + [\text{CO}_2]_{\text{g}}} \right) \quad (2)$$

where v and g refer to vesicles and glass, respectively.

Because there is a range of $\Delta_{\text{vapor-melt}}$ values from basaltic experiments (Javoy et al., 1978; Matthey, 1991; Matthey et al., 1990) and from observations (Aubaud et al., 2022), we use $\Delta_{\text{vapor-melt}}$ model values of 0 , $+2$ and $+4\text{\textperthousand}$ to estimate the $\delta^{13}\text{C}$ for the total CO_2 (vesicle+glass) of Loihi basalts.

A value of $\Delta_{\text{vapor-melt}} = 0$ would lead to all samples having a $\delta^{13}\text{C}$ of their total CO_2 equivalent to their measured vesicle $\delta^{13}\text{C}$. In this specific case, the distribution of total $\delta^{13}\text{C}$ values would be identical to the histogram shown in Fig. 3. A choice of $\Delta_{\text{vapor-melt}}$ consistent with the experimentally determined fractionation factors (for example, $+2$ and $+4\text{\textperthousand}$) will shift the total $\delta^{13}\text{C}$ downward from the vesicle $\delta^{13}\text{C}$ in a manner that is proportional to the fraction of CO_2 dissolved in the glass (Equation (2)).

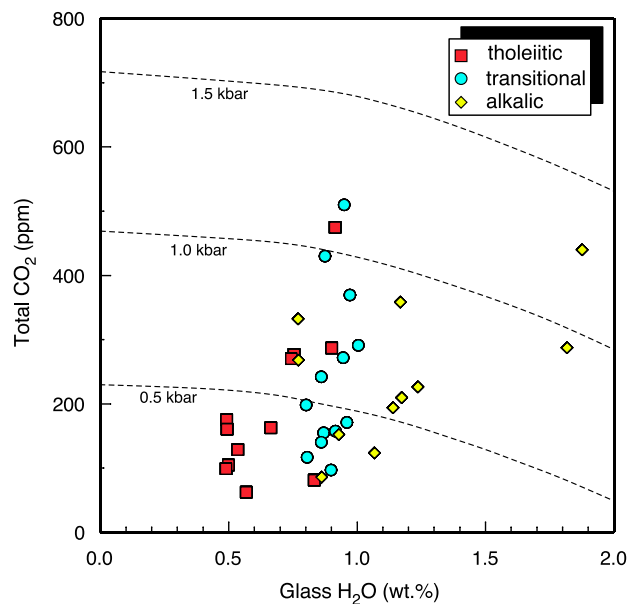


Fig. 5. Total (vesicles + glass) CO₂ vs. dissolved H₂O in Loihi basalts. Isobars are computed from VolatileCalc (Newman and Lowenstern, 2002).

When $\Delta_{\text{vapor-melt}}$ is chosen to be +2‰ or +4‰, respectively, the range for total $\delta^{13}\text{C}$ at Loihi seamount is -8.6 to -2.2‰ and -9.9 to -2.8‰. The median $\delta^{13}\text{C}$ for total CO₂ in each case is -3.9 and -5.2‰. Excluding the alkali basalts, given that they have experienced the most degassing, the total $\delta^{13}\text{C}$ in tholeiites and transitional basalts ranges from -7.0 to -2.2‰ (for $\Delta_{\text{vapor-melt}}$ of +2‰ to +4‰). Notably, tholeites from the north rift and east flank (Tunes 003D and Pisces 187-8) that have the highest ${}^3\text{He}/{}^4\text{He}$ ratios (30.6–31.9 R_A) have total $\delta^{13}\text{C} = -4 \pm 1\text{‰}$, even though their measured total CO₂ concentrations (100–175 ppm) are not among the most gas-rich of this study.

4.1.3. Magma degassing

The $\delta^{13}\text{C}$ estimated above for total CO₂ in Loihi basalts overlaps the range of $\delta^{13}\text{C}$ from -6 to -4‰ that is commonly attributed to the upper mantle, as deduced from the least degassed mid-ocean ridge basalts such as popping rocks (Pineau and Javoy, 1994; Cartigny et al., 2008), and for basalts from Midfell that show the least amount of degassing for Icelandic subglacial basalt glasses based on their He/Ar ratio (Barry et al., 2014). (Based on their geothermal fluid analyses, Barry et al., 2014 argued that the pre-eruptive $\delta^{13}\text{C}$ for basalts in Iceland was $-2.5 \pm 1.1\text{‰}$, and suggested that there may be a small difference in $\delta^{13}\text{C}$ between mantle plume sources and the depleted upper mantle source for MORBs. The least degassed subglacial basalt glass, from Midfell, has the heaviest $\delta^{13}\text{C}$, as expected with equilibrium degassing.) The total $\delta^{13}\text{C}$ values for Loihi basalts also overlap with $\delta^{13}\text{C}$ measured in summit crater fumaroles and hydrothermal fluids (-3.6 to -2.8‰) from nearby Kilauea (Gerlach and Taylor, 1991; Hilton et al., 1997). However, the major volatiles in the Loihi basalts record pressures <1.3 kbar (Fig. 5) and correspond to crustal equilibration depths from 0 to 3 km. These depths are significantly shallower than the dominant crystallization depth of 8–10 km inferred from petrologic modeling (Garcia et al., 2006) and shallower than seismically imaged features directly beneath the volcano, at 4–6 km in the crust (Merz et al., 2020) and near 50 km in the mantle (Wilding et al., 2023), where significant pre-eruptive loss of CO₂ may have occurred. The extensive degassing of CO₂ has increased the $\delta^{13}\text{C}$ of carbon left in the residual magma (see the next section), and any similarity of estimated $\delta^{13}\text{C}$ for total CO₂ in Loihi basalts to commonly accepted values for the upper mantle appears to be a coincidence.

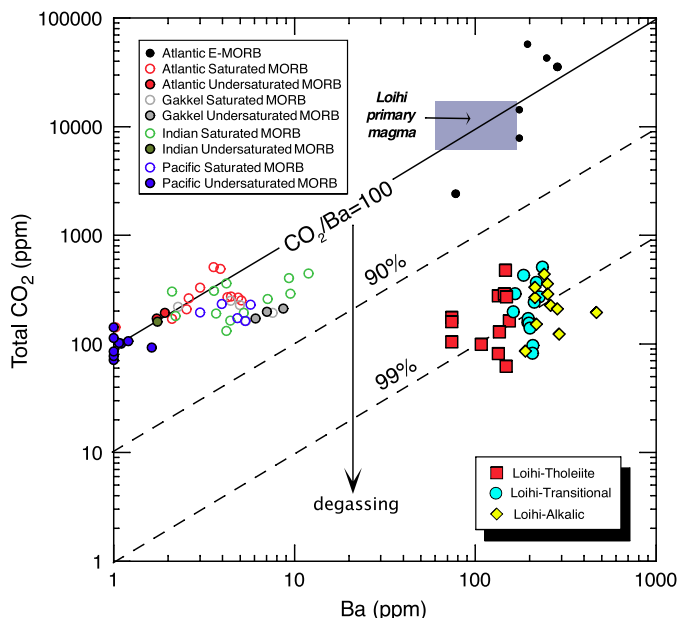


Fig. 6. Measured CO₂ vs. Ba in a variety of oceanic basalts. The mantle CO₂/Ba ratio varies between ~70–140. Rare examples of relatively undegassed basalts, such as E-MORB popping rocks and volatile undersaturated MORB glasses, have CO₂/Ba ratios consistent with this mantle range. Loihi basalts are highly degassed of their CO₂ relative to their inferred primary magmas, as estimated from crystal fractionation modeling and CO₂/Ba systematics. See text for further discussion.

Fig. 5 shows total CO₂ vs. dissolved H₂O in the Loihi basalts of this study. (Very little H₂O is degassed into vesicles due to its much higher solubility than CO₂). The general degassing path on this diagram is one where CO₂ decreases rapidly at higher pressure (greater depth) compared to H₂O, followed by an increasing trend to lower H₂O at lower pressure (shallower depth). Once vapor saturation is reached, bubbles of CO₂ form relatively deep. Most models predict that this degassing follows a near closed-system path – that is, the vapor bubbles are retained with the magma during ascent through the mantle and lithosphere (Dixon and Clague, 2001). When this vapor-saturated magma ponds for an extended time period, such as near the lithosphere-asthenosphere boundary or within the crust, significant gas loss occurs. Overall this leads to a quasi-closed system behavior that involves one or two periods of significant gas loss that may approximate isobaric bubble loss. Finally, when the magma ascends rapidly and is emplaced onto the seafloor, the last stage of degassing might also be influenced by open-system degassing or kinetic fractionation. Most gas loss during the evolution of Loihi magmas seems to have occurred during the earlier stage(s) under near equilibrium conditions. Kinetic fractionation appears to have been minor in affecting the basalt $\delta^{13}\text{C}$ (Fig. 4), although it may have affected the CO₂/ ${}^3\text{He}$ ratio (Fig. 2).

4.1.4. Reconstructing $\delta^{13}\text{C}$ of Loihi parental magmas

In this section we estimate the $\delta^{13}\text{C}$ of Loihi magmas prior to degassing. We first estimate the amount of CO₂ that was degassed for each basalt, by calculating the CO₂ concentrations in Loihi parental magmas using CO₂-trace element (Ba) systematics and crystal fractionation modeling (see the **Supplementary Information** for additional details). CO₂ concentrations at 18% MgO ranged from 0.65 – 1.9 wt.% (6535 to 18960 ppm). Comparing the estimated original CO₂ to the measured total (vesicle+dissolved) CO₂ concentrations reveals that the basalts are degassed of their initial CO₂ inventory by 96.7 to 99.4%, even for the very deeply erupted lavas along the south rift zone. Correcting for the amount of degassing for each basalt allows an estimate of its primary magma $\delta^{13}\text{C}$. **Fig. 6** summarizes these results on a CO₂ vs. Ba diagram.

Previous studies have shown that the mantle CO_2/Ba ratio has a value of ~ 70 -140 (Rosenthal et al., 2015; Michael and Graham, 2015; Le Voyer et al., 2017). Examples of relatively undegassed basalts, such as E-MORB popping rocks and volatile-undersaturated MORB glasses, have CO_2/Ba ratios consistent with this ratio of 70-140 (**Fig. 6**). The Ba concentrations in parental magmas at Loihi Seamount estimated using our crystallization model range from 60-175 ppm (**Fig. 6** and **Table S2** column P). Multiplying these Ba concentrations by a factor of 108 (Michael and Graham, 2015) provides an estimate for the parental magma CO_2 concentrations of 0.65 - 1.9 wt.% (**Fig. 6** and **Table S2** column T).

The $\delta^{13}\text{C}$ of the Loihi parental magmas may then be estimated through a choice of degassing model and the vapor - melt isotopic fractionation factor. Possible end-member models include closed-system degassing, open-system degassing, and kinetically controlled degassing. Depending on their ascent rate and storage times at depth, Loihi magmas might also have changed their style of degassing during the course of their evolution.

For a given value of $\Delta_{\text{vapor-melt}}$, open-system Rayleigh degassing leads to the most extreme C isotope estimates for a parental magma. During this type of degassing, a magma loses gas in infinitesimal increments above its vapor saturation threshold, with the vapor $\delta^{13}\text{C}$ composition controlled by the equilibrium value of $\Delta_{\text{vapor-melt}}$. Thus the residual magma continuously evolves in its $\delta^{13}\text{C}$ and can reach highly fractionated, low $\delta^{13}\text{C}$ compositions during open-system degassing. In closed-system degassing, the vapor and melt maintain isotopic equilibrium and the gas remains in contact with the magma. This type of behavior leads to less extreme fractionation and seems to approximate the evolution of Hawaiian magmas at Kilauea and Loihi (e.g., Gerlach and Taylor, 1991; Dixon and Clague, 2001). This approximate closed-system behavior takes place in one or more episodes of closed-system bubble growth and accumulation during magma ascent, separated by intervals of open-system behavior during which most of the vapor leaves the system (perhaps via isobaric bubble loss) such as during protracted storage of magma in the mantle and lithosphere (Dixon and Clague, 2001). Finally, in the very last stage of degassing - at very shallow depths during eruption - there could be some open-system (Rayleigh) degassing or potentially kinetic fractionation.

Regardless of the exact model choice of $\Delta_{\text{vapor-melt}}$, closed-system degassing projections from magmas having low total CO_2 (<500 ppm) and $\delta^{13}\text{C}$ values of -5 to $-2\text{\textperthousand}$, to parental magmas that have high CO_2 concentrations as we infer for Loihi basalts, indicate those parental magma $\delta^{13}\text{C}$ values are -4 to $+1\text{\textperthousand}$ (**Table S2**). Furthermore, the exact choice of CO_2/Ba ratio of 108 - as opposed to alternative values of 70 or 140 - has nearly a negligible effect - typically $< 0.1\text{\textperthousand}$ - on the estimated $\delta^{13}\text{C}$ of the primary magmas.

Open-system degassing may be a more appropriate model for a few of the basalts, particularly some of the alkalic lavas given their lower and more variable $\delta^{13}\text{C}$ (**Table S1**, **Figs. 3, S1**). Open-system degassing would lead to even higher estimates of $\delta^{13}\text{C}$ for the parental magma. Also, if a $\Delta_{\text{vapor-melt}} = 0\text{\textperthousand}$ is assumed (which is not representative of most samples, but which would apply if partial kinetic fractionation had occurred), this still leads to parental magma $\delta^{13}\text{C} = -2\text{\textperthousand}$ for some of the Loihi basalts, which is outside the prevalent mantle range.

By making an appropriate choice of $\Delta_{\text{vapor-melt}}$ and projecting each sample along a closed-system path back to its parental magma CO_2 , one can obtain a petrologically consistent value of its $\delta^{13}\text{C}$. A choice of $\Delta_{\text{vapor-melt}} = +2\text{\textperthousand}$, which seems to approximately describe the behavior for many of the Loihi basalts (**Fig. S1**), leads to parental magma $\delta^{13}\text{C}$ values between -4.3 and $-0.20\text{\textperthousand}$ (**Table S2** column V), with a median of $-1.9\text{\textperthousand}$ (excluding a single basanite sample, Pisces 158-4). A choice of $\Delta_{\text{vapor-melt}} = +4\text{\textperthousand}$

leads to parental magma $\delta^{13}\text{C}$ values that are even higher, between -3.9 and $+1.1\text{\textperthousand}$ (**Table S2** column W), with a median of $-1.3\text{\textperthousand}$. Using an open-system degassing model would lead to even higher estimates of $\delta^{13}\text{C}$ for the parental magma.

It is noteworthy that high concentrations of CO_2 , accompanied by elevated $\delta^{13}\text{C}$, have been inferred for the primary magmatic gas at other ocean island hotspots. Based on analyses of olivine-hosted melt inclusions for Réunion Island basalts, primary magmatic $[\text{CO}_2]$ ranges up to 3.5 ± 1.4 wt.% at Piton de la Fournaise, with $\delta^{13}\text{C} = -0.8 \pm 1\text{\textperthousand}$ (Bouduire et al., 2018). Based on analyses of fluid inclusions in the olivine and pyroxene of xenoliths from El Hierro (Canary Islands), primary magmatic $\delta^{13}\text{C} = -2.4$ to $+1\text{\textperthousand}$ (Sandoval-Velasquez et al., 2021). Elevated $\delta^{13}\text{C}$ is a feature of ocean island hotspot mantle sources, and so of general significance for the deep carbon cycle.

In summary, Loihi parental magmas, and by inference the Loihi mantle plume source, have $\delta^{13}\text{C}$ values that are significantly heavier (by about $3\text{-}5\text{\textperthousand}$) than the commonly accepted values of -6 to $-4\text{\textperthousand}$ for the upper mantle. Details of the quasi closed-system degassing history, and the initial CO_2 contents of primary magma remain uncertain, but they do not dramatically alter this conclusion.

4.2. Hypotheses for the origin of elevated $\delta^{13}\text{C}$ in the Loihi mantle plume

Fig. 7 shows $^3\text{He}/^4\text{He}$ of Loihi basalts against the computed parental magma $\delta^{13}\text{C}$. The median parental magma $\delta^{13}\text{C} = -1.9\text{\textperthousand}$ in this example. The diagram was constructed assuming closed-system degassing, using $\Delta_{\text{vapor-melt}} = +2\text{\textperthousand}$, both 1) when computing total $\delta^{13}\text{C}$ in the erupted magma from the measured vesicle $\delta^{13}\text{C}$, and 2) when projecting back to the undegassed parental magma (18 wt.% MgO) using the petrologic modeling estimate of its Ba content and $\text{CO}_2/\text{Ba} = 108$. Below we discuss possible scenarios for the origin of $\delta^{13}\text{C}$ in the Loihi mantle source that is elevated above typical mantle values.

4.2.1. Primordial $\delta^{13}\text{C}$ heterogeneity in Earth's mantle

One important question is whether or not the elevated Loihi $\delta^{13}\text{C}$ values indicate contribution from primordial mantle. Terrestrial bulk N and H isotope compositions overlap the range of compositions seen in some carbonaceous chondrites (CCs), suggesting that many volatile species on Earth were sourced from material similar to that which formed CC parent bodies (Marty, 2012). Meteoritic bulk carbon (**Fig. S2**) shows an extremely large range of $\delta^{13}\text{C}$ (Alexander et al., 2012) and thus seems to allow for some (currently unknown) degree of heterogeneity in primordial $\delta^{13}\text{C}$ of Earth's mantle. Carbon isotopes in unbrecciated ureilites (carbon-rich ultramafic achondrites that represent mantle fragments of a differentiated parent body) also vary from -8.5 to $+0.4\text{\textperthousand}$ (Barrat et al., 2017). The inferred Loihi source $\delta^{13}\text{C}$ values of -4 to $+0.8\text{\textperthousand}$ might therefore be a relict feature of deep, primitive mantle. Admittedly though, the meteorite data alone do not provide a unique constraint on Earth's primordial carbon isotope values (see further discussion in **Supplementary Information**).

An additional line of evidence for possible primordial heterogeneity in $\delta^{13}\text{C}$ of the mantle comes from diamonds. Diamonds are unambiguously of mantle origin, and those with peridotitic inclusions mostly show $\delta^{13}\text{C}$ between -2 and $-8\text{\textperthousand}$ with a mode near $-6\text{\textperthousand}$, similar to mid-ocean ridge basalts (Cartigny et al., 2014). Other diamonds contain mineral inclusions that indicate diamond growth occurred in the lower mantle. A notable case is the Kankan diamonds from Guinea (Palot et al., 2012). Palot et al. (2012) excluded two analyses that they were not able to replicate for Kankan diamonds (for which they measured $\delta^{13}\text{C}$ values of $+0.1$ and $+1.4\text{\textperthousand}$). Even excluding those data, the range

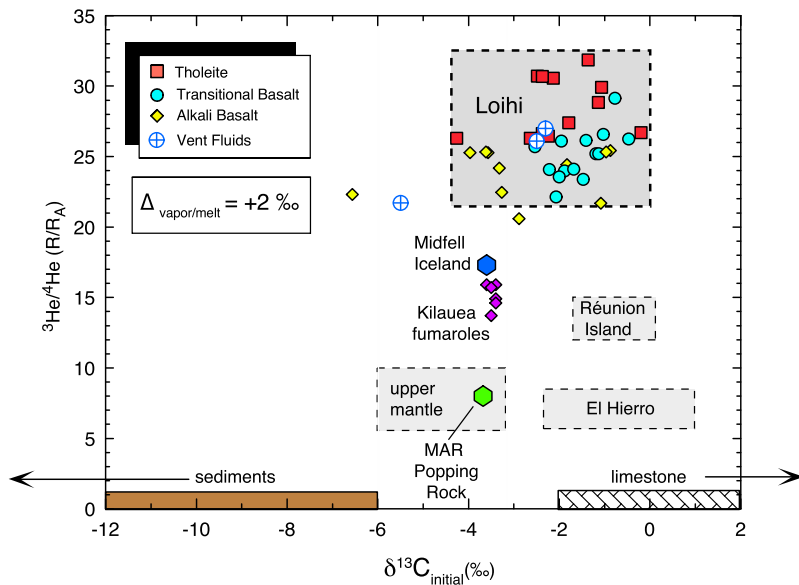


Fig. 7. Vesicle ${}^3\text{He}/{}^4\text{He}$ vs. $\delta^{13}\text{C}$. Loihi parental magma $\delta^{13}\text{C}$ values were estimated using $\Delta_{\text{vapor-melt}} = +2\text{\textperthousand}$, and projection to initial $[\text{CO}_2]$ based on crystal fractionation modeling and $\text{CO}_2/\text{Ba}=108$ (see main text and supplementary material for discussion). The outlined box shows the range of He and C isotope values for Loihi tholeites and transitional basalts; alkali basalts extend to lower values of $\delta^{13}\text{C}$ and ${}^3\text{He}/{}^4\text{He}$. Also shown are measured values for Loihi vent fluids (Sedwick et al., 1994), Kilauea fumaroles (Hilton et al., 1997), Midfjall in Iceland (Barry et al., 2014), and Mid-Atlantic Ridge popping rock (Pineau and Javoy, 1994). The range of $\delta^{13}\text{C}$ for upper mantle-derived magmas before degassing is -6 to $-3.2\text{\textperthousand}$, with a ${}^3\text{He}/{}^4\text{He}$ range of 6 – 10 R_A (Graham et al., 2014; Graham and Michael, 2021). The ranges inferred for primary CO_2 gas at Réunion Island and El Hierro (Canary Islands) based on melt inclusion analyses from olivine and pyroxene are from Boudoire et al. (2018) and Sandoval-Velasquez et al. (2021), respectively.

in Kankan diamonds is -4.3 to $-1.4\text{\textperthousand}$. This range overlaps significantly with that inferred for the Loihi mantle source region (-4.2 to $+0.8\text{\textperthousand}$). We conclude that there is some circumstantial evidence from ultra-deep diamonds for possible primordial heterogeneity in mantle $\delta^{13}\text{C}$ similar to the range implied by the new Loihi basalt $\delta^{13}\text{C}$ data. However, whether or not this heterogeneity in diamond $\delta^{13}\text{C}$ relates to the time of Earth's accretion is not known. Some ultra-deep diamonds contain carbonate inclusions, and Shirey et al. (2019) suggested that $\delta^{13}\text{C}$ values of the Kankan diamonds record the involvement of subducted carbonate with little or no organic carbon involved.

4.2.2. Tectonically recycled carbon in the Hawaiian mantle plume

Carbonate may be recycled to the mantle both in marine sediments and as carbonate minerals precipitated in altered oceanic crust (AOC). The carbonate of AOC can have highly variable $\delta^{13}\text{C}$ ranging from -24 to $+11\text{\textperthousand}$, it contributes a sub-equal proportion to the total subducted C flux, and it potentially survives to greater depth after subduction than sedimentary carbonate (Li et al., 2019). Mixing in the deep mantle between recycled sedimentary carbonate and pristine plume material (chosen to have high ${}^3\text{He}/{}^4\text{He}$ and typical mantle $\delta^{13}\text{C} = -6\text{\textperthousand}$ as one example) would lead to lower ${}^3\text{He}/{}^4\text{He}$ at higher values of $\delta^{13}\text{C}$. Such a binary mixing curve would show a strong, concave downward curvature on Fig. 7 due to the very large enrichment in C and the low ${}^3\text{He}/{}^4\text{He}$ of the carbonate. The data in Fig. 7 do not show a clear trend. Loihi transitional basalts and many of the tholeites may actually show a tendency to slightly higher $\delta^{13}\text{C}$ at higher ${}^3\text{He}/{}^4\text{He}$. However, the data scatter makes it difficult to rule out that such mixing has occurred.

A simple mixing calculation reveals that only a very small mass fraction of recycled sedimentary CaCO_3 is needed to account for the shift in $\delta^{13}\text{C}$ of Loihi basalts. The amount of recycled material depends on assumptions for the compositions of both the pristine and recycled end-members. One example is depicted in Fig. 8. It assumes binary mixing, between pristine mantle having $\delta^{13}\text{C} = -6\text{\textperthousand}$ and $[\text{C}] = 100 \text{ ppm}$ (366 ppm CO_2), and recycled CaCO_3 having $\delta^{13}\text{C} = 0\text{\textperthousand}$. These model values are a reasonable choice given

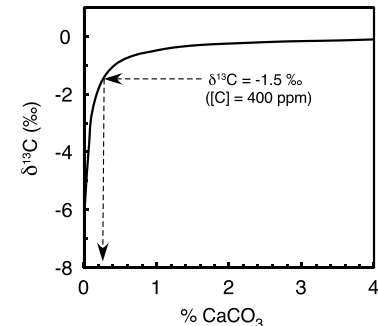


Fig. 8. $\delta^{13}\text{C}$ vs. mass of CaCO_3 in the mantle source, showing one model mixing curve. The model assumes binary mixing between pristine mantle having $\delta^{13}\text{C} = -6\text{\textperthousand}$ and $[\text{C}] = 100 \text{ ppm}$ (366 ppm CO_2), and recycled CaCO_3 having $\delta^{13}\text{C} = 0\text{\textperthousand}$. As one example, when this mixture has $\delta^{13}\text{C} = -1.5\text{\textperthousand}$, it will have $[\text{C}] = 400 \text{ ppm}$, and its mantle source contains 0.25% CaCO_3 as shown by the arrow.

that the $\delta^{13}\text{C}$ of limestone has not varied markedly for most of Earth's history (e.g., Hayes and Waldbauer, 2006), and that much of the mantle (assumed here to be unaffected by recycling) is inferred to have C concentrations on the order of 25 – 100 ppm (90 – 365 ppm CO_2) and $\delta^{13}\text{C}$ of -6 to $-4\text{\textperthousand}$ (e.g., Javoy et al., 1986; Deines, 2002; Cartigny et al., 2013; Le Voyer et al., 2017). Based on such a simple mixing model, only a very small mass fraction of recycled CaCO_3 can be present in the Loihi mantle source. For example, $\sim 0.25\%$ CaCO_3 would be involved when both $\delta^{13}\text{C} = -1.5\text{\textperthousand}$ (similar to the median Loihi source value deduced earlier) and $[\text{CO}_2] = 1467 \text{ ppm}$ ($[\text{C}] = 400 \text{ ppm}$, similar to the source deduced from Hawaiian melt inclusions; Tucker et al., 2019). Furthermore, although this represents a small mass fraction of the plume, the recycled carbon makes up the dominant proportion (75%) of the plume carbon in this example. Other end-member choices in the simple mixing model are discussed in the **Supplementary Information**. We conclude that any reasonable choice of model values requires only a small mass fraction of carbonate (<1%) in the Loihi plume source to account for the $\delta^{13}\text{C}$ observations.

Notably, there is additional evidence for the presence of small amounts of recycled CaCO_3 in the Hawaiian plume source. Huang et al. (2011) suggested as much as 4% carbonate was present in the mantle source of Makapuu-stage lavas from the Koolau shield of Oahu, which show elevated Sr/Nb and $^{44}\text{Ca}/^{40}\text{Ca}$ ratios that are 0.3‰ lower than other shield lavas from Hawaii. Sobolev et al. (2011) inferred that a small amount of recycled marine carbonate was present in the Hawaiian mantle source based on a comparison of Sr isotopes in Mauna Loa melt inclusions with the record of $^{87}\text{Sr}/^{86}\text{Sr}$ in Phanerozoic limestone.

Pietruszka et al. (2013) showed from Sr-Nd-Pb and trace element systematics that as much as ~8–15% altered (and dehydrated) ocean crust (AOC) may be present within the Loihi mantle plume. Carbonate veins precipitated during low temperature (~10 °C) hydrothermal circulation may comprise as much as 1–3% by volume in the upper 1 km of slow spreading crust (Alt and Teagle, 1999; Shilobreeva et al., 2011; Martinez et al., 2021), while in fast spreading crust the volume percentage is typically an order of magnitude less (Gillis and Coogan, 2011). If 8–15% AOC is present within the Loihi mantle plume (Pietruszka et al., 2013), our estimate of ~0.25% carbonate would constitute 1.5–3% of the AOC if all the carbonate was present as secondary veins. The $\delta^{13}\text{C}$ of inorganic C precipitated in the upper 300 m of the AOC varies from −0.4 to +1.5‰ in 170 Ma altered basalts in the western Pacific (Martinez et al., 2021), and overlaps with the highest $\delta^{13}\text{C}$ values in the Loihi mantle source region. We simply note that an estimate of ~0.25% recycled carbonate seems to be of the same order of magnitude when compared to the amount of carbonate veining that would be present if the Loihi plume contains ~8–15% AOC.

4.2.3. Carbon from Earth's core

The Hawaiian hotspot is underlain by a laterally extensive (~900 km diameter) ultra-low velocity zone (ULVZ) at the core-mantle boundary (Cottaar and Romanowicz, 2012). ULVZs are thin (order of 10–20 km high) patches that lie directly on the CMB. They may have originated either as Fe-rich melts crystallized from a magma ocean (Labrosse et al., 2007), or by chemical enrichment from the outer core through enhanced grain-boundary fluxes (Hayden and Watson, 2007). ^{182}W anomalies in high- $^3\text{He}/^4\text{He}$ basalts have been interpreted to originate from core-mantle interaction (Mundl-Petermeier et al., 2020), and grain boundary diffusion of carbon in this region of the mantle may lead to a flux of carbon from the outer core to the overlying mantle (Hayden and Watson, 2008). It is reasonable to ask whether such processes may have led to ^{13}C enrichment of the Loihi mantle source. Carbon isotope fractionation between solid carbon and Fe-carbide melts has been studied experimentally, and it shows that the metallic phase will be enriched in ^{12}C (Satish-Kumar et al., 2011). Furthermore, in iron meteorites that represent fragments of ancient core material from planetary parent bodies, the C isotope composition of iron bearing phases such as cohenite $(\text{FeNiCo})_3\text{C}$ is enriched in ^{12}C compared to coexisting graphite (Deines and Wickman, 1975). These observations seem to eliminate the possibility that elevated $\delta^{13}\text{C}$ values of the Loihi mantle source originate by bulk transfer of carbon from the core. However, if carbon exchange occurs between the metallic core and silicates within the ULVZs at the CMB, it might lead to higher $\delta^{13}\text{C}$ in the ULVZs compared to the ambient mantle due to preferential ^{12}C partitioning into the core.

4.3. Primordial vs. recycled carbon in the source of mantle plumes

There is mounting evidence that recycled surficial carbonate is present in mantle hotspot source regions. Recent studies of stable isotopic systems such as Zn and Ca seem to point to deeply recycled carbonate in the plume source of some ocean island basalts (Zhang et al., 2022; Huang et al., 2011). Recycled carbonate has

also been suggested to lead to the distinct radiogenic Pb isotope compositions of HIMU island localities such as St. Helena, Mangaia and Tubuai (Castillo et al., 2018).

When sedimentary carbonate in oceanic crust is subducted into the mantle it is not expected to survive decarbonation reactions that occur at depths >1500 km (Drewitt et al., 2019). Instead, most if not all of the subducted carbonate will be transformed into refractory diamond in the lowermost mantle. The high carbon contents of some OIBs and melt inclusions (Tucker et al., 2019) might therefore be attributed to deeply recycled oceanic crust that contains diamond in the mantle source. During plume upwelling this carbon is expected to oxidize and become carbonate that will ultimately be incorporated into OIB melts (Drewitt et al., 2019). Carbonate may also form through oxidation of primordial carbon that is present as diamond in the plume, once plume material is transported to mantle transition zone depths (Sun et al., 2018). This transformation can also lead to ^{13}C enrichment in the carbonate, because even at 1800 °C within the mantle transition zone the equilibrium $\delta^{13}\text{C}$ of carbonate is ~1‰ heavier than diamond (Cartigny et al., 2014).

These processes and our current lack of knowledge of Earth's initial carbon isotope composition are fundamental limitations in assessing the importance of primordial vs. recycled carbon in Earth's interior from carbon isotope variations. Although the $\delta^{13}\text{C}$ values for the high- $^3\text{He}/^4\text{He}$ basalts of this study do not unambiguously discriminate between deeply derived primordial carbon (having median $\delta^{13}\text{C}$ near −1.5‰) vs. surficial carbonate that has been tectonically recycled (having $\delta^{13}\text{C} \geq 0\text{\textperthousand}$), they are consistent with the presence of ~10% recycled altered oceanic crust within the Loihi mantle plume. The development and analyses of other sensitive geochemical tracers of recycled surficial carbonate and primordial mantle material are needed for Hawaiian basalts.

5. Conclusions

The $\delta^{13}\text{C}$ of vesicle CO_2 in Loihi basalts ranges from −7 to −1‰, with a median $\delta^{13}\text{C} = -2.5\text{\textperthousand}$. Loihi magmas appear to have followed a quasi closed-system degassing path for most of their evolution. Estimates of the parental magma $\delta^{13}\text{C}$ corrected for this degassing range from −4 to +1‰, with a median value of −1.5‰. This range is higher than values of −3.5 to −6‰ for mantle-derived basalts and most peridotitic diamonds. This difference could be ascribed to primordial heterogeneity of $\delta^{13}\text{C}$ in the bulk silicate Earth. Another possible explanation may be exchange of carbon at the core-mantle boundary between ultra-low velocity zone silicates and the liquid outer core. Alternatively, it may be due to a small mass fraction (<1%) of surficial carbonate that was tectonically recycled into the Loihi plume source region.

Additional measurements of $\delta^{13}\text{C}$ for the dissolved (glass) carbon in Loihi basalts are needed to further evaluate magmatic degassing and the carbon isotope composition of the mantle plume source. The results of the present study suggest that two volatile elements (helium and carbon) might have different sources (primordial vs. recycled) within a single mantle plume. A more comprehensive characterization of carbon isotope variations, coupled with radiogenic and stable isotopes of other elements on the same suites of ocean island basalts, is needed to fully assess the relative importance of recycled vs. primordial material in deep mantle source regions.

CRediT authorship contribution statement

David W. Graham: Conceptualization, Data curation, Formal analysis, Investigation, Methodology, Visualization, Writing – original draft, Writing – review & editing. **Peter J. Michael:** Conceptualization, Data curation, Formal analysis, Investigation, Methodology,

Visualization, Writing – review & editing. **Thi B. Truong:** Data curation, Formal analysis, Investigation, Visualization, Writing – review & editing.

Declaration of competing interest

The authors declare that they have no known competing financial interests or personal relationships that could have appeared to influence the work reported in this paper.

Data availability

All data used in this study are included in the supplementary material. Additional data are available at <https://doi.org/10.26022/IEDA/112511> (Graham, D., Michael, P.J., Truong, T.B., Garcia, M.O., 2024. Helium and carbon isotopes, volatiles, and trace elements in submarine basalt glasses from Loihi Seamount, version 1.0. Interdisciplinary Earth Data Alliance (IEDA)).

Acknowledgements

We thank Mike Garcia for graciously providing Loihi basalt glass samples, sharing data, and his help with sample selection. Transport and curation of Loihi Seamount samples at the University of Hawaii was supported by grant OCE17-37284 to Mike Garcia. The Smithsonian Institution provided KK series samples with the valuable assistance of Leslie Hale. We are indebted to Andy Ross for his expertise in making the $\delta^{13}\text{C}$ measurements with the MAT 253 mass spec. We thank Chris Russo for guidance in making the laser ablation ICP-MS measurements in the Keck Lab for Plasma Spectrometry, and Cory Langhoff for expertise in constructing the sample map. We thank Bill White and an anonymous reviewer for providing constructive comments and suggestions that improved the manuscript. This study was supported by the Marine Geology & Geophysics Program at the National Science Foundation, through grants OCE17-63255 (DG) and OCE17-63259 (PM). Additional support was provided by the McMan endowment of The University of Tulsa.

Appendix A. Supplementary material

Supplementary material related to this article can be found online at <https://doi.org/10.1016/j.epsl.2023.118248>.

References

Alexander, C.M.O.D., Bowden, R., Fogel, M.L., Howard, K.T., Herd, C.D.K., Nittler, L.R., 2012. The provenances of asteroids, and their contributions to the volatile inventories of the terrestrial planets. *Science* 337, 721–723.

Alt, J.C., Teagle, D.A.H., 1999. The uptake of carbon during alteration of ocean crust. *Geochim. Cosmochim. Acta* 63, 1527–1535.

Anderson, K.R., Poland, M.P., 2017. Abundant carbon in the mantle beneath Hawai'i. *Nat. Geosci.* <https://doi.org/10.1038/NGEO3007>.

Aubaud, C., 2022. Carbon stable isotope constraints on CO_2 degassing models of ridge, hotspot and arc magmas. *Chem. Geol.* 605, 120962.

Barrat, J.-A., Sansjøfro, P., Yamaguchi, A., Greenwood, R.C., Gillet, P., 2017. Carbon isotopic variation in ureilites: evidence for an early, volatile-rich inner Solar System. *Earth Planet. Sci. Lett.* 478, 143–149.

Barry, P.H., Hilton, D.R., Füri, E., Halldorsson, S.A., Gronvold, K., 2014. Carbon isotope and abundance systematics of Icelandic geothermal gases, fluids and subglacial basalts with implications for mantle plume-related CO_2 fluxes. *Geochim. Cosmochim. Acta* 134, 74–99.

Boudoire, G., Rizzo, A.L., Di Muro, A., Grassia, F., Liuzzo, M., 2018. Extensive CO_2 degassing in the upper mantle beneath oceanic basaltic volcanoes: first insights from Piton de la Fournaise volcano (La Réunion Island). *Geochim. Cosmochim. Acta* 235, 376–401.

Carmichael, I.S.E., Turner, F.J., Verhoogen, J., 1974. Igneous and Metamorphic Petrology. McGraw-Hill.

Cartigny, P., Palot, M., Thomassot, E., Harris, J.W., 2014. Diamond formation: a stable isotope perspective. *Annu. Rev. Earth Planet. Sci.* 42, 699–732.

Cartigny, P., Pineau, F., Aubaud, C., Javoy, M., 2008. Towards a consistent mantle carbon flux estimate: insights from volatile systematics ($\text{H}_2\text{O}/\text{Ce}$, δD , CO_2/Nb) in the North Atlantic mantle. *Earth Planet. Sci. Lett.* 265, 672–685.

Castillo, P.R., MacIsaac, C., Perry, S., Veizer, J., 2018. Marine carbonates in the mantle source of oceanic basalts: Pb isotopic constraints. *Nature Sci. Rep.* 8, 14932.

Cottaar, S., Romanowicz, B., 2012. An unusually large ULVZ at the base of the mantle near Hawaii. *Earth Planet. Sci. Lett.* 355–356, 213–222.

Craig, H., 1987. Comment on “Carbon isotope systematics of a mantle hotspot: a comparison of Loihi seamount and MORB glasses” by R.A. Exley, D.P. Mattey, D.A. Clague and C.T. Pillinger. *Earth Planet. Sci. Lett.* 82, 384–386.

Deines, P., 2002. The carbon isotope geochemistry of mantle xenoliths. *Earth-Sci. Rev.* 58, 247–278.

Deines, P., Wickman, F.E., 1975. A contribution to the stable isotope geochemistry of iron meteorites. *Geochim. Cosmochim. Acta* 39, 547–557.

Dixon, J.E., Clague, D.A., 2001. Volatiles in basaltic glasses from Loihi Seamount, Hawaii: evidence for a relatively dry plume component. *J. Petrol.* 42, 627–654.

Drewitt, J.W.E., Walter, M.J., Zhang, H., McMahon, S.C., Edwards, D., Heinen, B.J., Lord, O.T., Zanzellini, S., Kleppe, A.K., 2019. The fate of carbonate in oceanic crust subducted into Earth's lower mantle. *Earth Planet. Sci. Lett.* 511, 213–222.

Exley, R.A., Mattey, D.P., Clague, D.A., Pillinger, C.T., 1986. Carbon isotope systematics of a mantle “hotspot”: a comparison of Loihi Seamount and MORB glasses. *Earth Planet. Sci. Lett.* 78, 189–199.

Garcia, M.O., Caplan-Auerbach, J., De Carlo, E.H., Kurz, M.D., Becker, N., 2006. Geology, geochemistry and earthquake history of Loihi Seamount, Hawaii's youngest volcano. *Chem. Erde* 66, 81–108.

Garcia, M.O., Foss, D.J.P., West, H.B., Mahoney, J.J., 1995. Geochemical and isotopic evolution of Loihi Volcano, Hawaii. *J. Petrol.* 36, 1647–1674.

Gerlach, T.M., Taylor, B.E., 1991. Carbon isotope constraints on degassing of carbon dioxide from Kilauea Volcano. *Geochim. Cosmochim. Acta* 54, 2051–2058.

Gillis, K.M., Coogan, L.A., 2011. Secular variation in carbon uptake into the ocean crust. *Earth Planet. Sci. Lett.* 302, 385–392.

Graham, D.W., Hanan, B.B., Hémond, C., Blichert-Toft, J., Albarède, F., 2014. Helium isotopic textures in Earth's upper mantle. *Geochem. Geophys. Geosyst.* 15, 2048–2074.

Graham, D.W., Michael, P.J., 2021. Predominantly recycled carbon in Earth's upper mantle revealed by $\text{He}-\text{CO}_2-\text{Ba}$ systematics in ultradepleted ocean ridge basalts. *Earth Planet. Sci. Lett.* 554, 116646.

Gülcher, A.P., Ballmer, M.D., Tackley, P.J., 2021. Coupled dynamics and evolution of primordial and recycled heterogeneity in Earth's lower mantle. *Solid Earth* 12, 2087–2107.

Hayden, L.A., Watson, E.B., 2007. A diffusion mechanism for core–mantle interaction. *Nature* 450, 709–712.

Hayden, L.A., Watson, E.B., 2008. Grain boundary mobility of carbon in Earth's mantle: a possible carbon flux from the core. *Proc. Natl. Acad. Sci.* 105, 8537–8541.

Hayes, J.M., Waldbauer, J.R., 2006. The carbon cycle and associated redox processes through time. *Philos. Trans. R. Soc. Lond. B* 361, 931–950.

Hilton, D.R., McMurtry, G.M., Kreulen, R., 1997. Evidence for extensive degassing of the Hawaiian mantle plume from helium–carbon relationships at Kilauea volcano. *Geophys. Res. Lett.* 24, 3065–3068.

Honda, M., McDougall, I., Patterson, D.B., Doulgeris, A., Clague, D.A., 1993. Noble gases in submarine pillow basalt glasses from Loihi and Kilauea, Hawaii: a solar component in the Earth. *Geochim. Cosmochim. Acta* 57, 859–874.

Huang, S., Farkas, J., Jacobsen, S.B., 2011. Stable calcium isotopic compositions of Hawaiian shield lavas: evidence for recycling of ancient marine carbonates into the mantle. *Geochim. Cosmochim. Acta* 75, 4987–4997.

Javoy, M., Pineau, F., Liyama, I., 1978. Experimental determination of the isotopic fractionation between gaseous CO_2 and carbon dissolved in tholeiitic magma. *Contrib. Mineral. Petrol.* 67, 35–39.

Javoy, M., Pineau, F., Delorme, H., 1986. Carbon and nitrogen isotopes in the mantle. *Chem. Geol.* 57, 41–62.

Kaneoka, I., Hanyu, T., Yamamoto, J., Miura, Y., 2002. Noble gas systematics of the Hawaiian volcanoes based on the analysis of Loihi, Kilauea and Koolau submarine rocks. In: Hawaiian Volcanoes: Deep Underwater Perspectives. American Gophys Union, pp. 373–389.

Kurz, M.D., Jenkins, W.J., Hart, S.R., 1982. Helium isotopic systematics of oceanic islands and mantle heterogeneity. *Nature* 297, 43–46.

Kurz, M.D., Jenkins, W.J., Hart, S.R., Clague, D., 1983. Helium isotopic variations in the volcanic rocks from loihi seamount and the island of Hawaii. *Earth Planet. Sci. Lett.* 66, 388–406.

Labrosse, S., Hernlund, J., Coltice, N., 2007. A crystallizing dense magma ocean at the base of the Earth's mantle. *Nature* 450, 866–870.

Le Voyer, M., Kelley, K.A., Cottrell, E., Hauri, E.H., 2017. Heterogeneity in mantle carbon content from CO_2 -undersaturated basalts. *Nat. Commun.*

Li, K., Li, L., Pearson, D.G., Stachel, T., 2019. Diamond isotope compositions indicate altered igneous oceanic crust dominates deep carbon recycling. *Earth Planet. Sci. Lett.* 516, 190–201.

Li, M., McNamara, A.K., Garnero, E.J., 2014. Chemical complexity of hotspots caused by cycling oceanic crust through mantle reservoirs. *Nat. Geosci.* 7, 366–370.

Loewen, M., Graham, D.W., Bindeman, I.N., Lupton, J.E., Garcia, M.O., 2019. Hydrogen isotopes in high $^3\text{He}/^4\text{He}$ submarine basalts: primordial vs. recycled water and the veil of mantle enrichment. *Earth Planet. Sci. Lett.* 508, 62–73.

Martinez, I., Shilobreeva, S., Alt, J.C., Polyakov, V., Agrinier, P., 2021. The origin and fate of C during alteration of the oceanic crust. *C. R. Géosci.* 353, 319–336.

Marty, B., 2012. The origins and concentrations of water, carbon, nitrogen and noble gases on Earth. *Earth Planet. Sci. Lett.* 313–314, 56–66.

Marty, B., Jambon, A., 1987. $C/^{3}He$ in volatile fluxes from the solid Earth: implications for carbon geodynamics. *Earth Planet. Sci. Lett.* 83, 16–26.

Mattey, D.P., 1991. Carbon dioxide solubility and carbon isotope fractionation in basaltic melt. *Geochim. Cosmochim. Acta* 55, 3467–3473.

Mattey, D.P., Taylor, W., Green, D.H., Pillinger, C.T., 1990. Carbon isotopic fractionation between CO_2 vapour, silicate and carbonate melts: an experimental study to 30 kbar. *Contrib. Mineral. Petrol.* 104, 492–505.

McNamara, A.K., 2019. A review of large low shear velocity provinces and ultra low velocity zones. *Tectonophysics* 760, 199–220.

Merz, D.K., Capelan-Auerbach, J., Thurber, C.H., 2020. Seismicity and velocity structure of Lō'ihi submarine volcano and southeastern Hawai'i. *J. Geophys. Res.* 124, 11380–11393.

Michael, P.J., Graham, D.W., 2015. The behavior and concentration of CO_2 in the suboceanic mantle: inferences from undegassed ocean ridge and ocean island basalts. *Lithos* 236–237, 338–351.

Mundl-Petermeier, A., Walker, R.J., Fischer, R.A., Lekic, V., Jackson, M.G., Kurz, M.D., 2020. Anomalous ^{182}W in high $^{3}He/^{4}He$ ocean island basalts: fingerprints of Earth's core? *Geochim. Cosmochim. Acta* 271, 194–211.

Newman, S., Lowenstern, J.B., 2002. VolatileCalc: a silicate melt- H_2O - CO_2 solution model written in Visual Basic for Excel. *Comput. Geosci.* 28, 597–604.

Palot, M., Cartigny, P., Harris, J.W., Kaminsky, F.V., Stachel, T., 2012. Evidence for deep mantle convection and primordial heterogeneity from nitrogen and carbon stable isotopes in diamond. *Earth Planet. Sci. Lett.* 357–358, 179–193.

Pietruszka, A.J., Keyes, M.J., Duncan, J.A., Hauri, E.H., Carlson, R.W., Garcia, M.O., 2011. Excess of seawater-derived ^{234}U in volcanic glasses from Loihi Seamount due to crustal contamination. *Earth Planet. Sci. Lett.* 304, 280–289.

Pietruszka, A.J., Norman, M.D., Garcia, M.O., Marske, J.P., Burns, D.H., 2013. Chemical heterogeneity in the Hawaiian mantle plume from the alteration and dehydration of recycled oceanic crust. *Earth Planet. Sci. Lett.* 361, 298–309.

Pineau, F., Javoy, M., 1994. Strong degassing at ridge crests: the behaviour of dissolved carbon and water in basalt glasses at $14^{\circ}N$, Mid-Atlantic Ridge. *Earth Planet. Sci. Lett.* 123, 179–198.

Rison, W., Craig, H., 1983. Helium isotopes and mantle volatiles in Loihi Seamount and Hawaiian Island basalts and xenoliths. *Earth Planet. Sci. Lett.* 66, 407–426.

Rosenthal, A., Hauri, E.H., Hirschmann, M.M., 2015. Experimental determination of C, F, and H partitioning between mantle minerals and carbonated basalt, CO_2/Ba and CO_2/Nb systematics of partial melting, and the CO_2 contents of basaltic source regions. *Earth Planet. Sci. Lett.* 412, 77–87.

Sandoval-Velasquez, A., Rizzo, A.L., Aiuppa, A., Remigi, S., Padrón, E., Pérez, N.M., Frezzotti, M.L., 2021. Recycled crustal carbon in the depleted mantle source of El Hierro volcano, Canary Islands. *Lithos* 400–401, 106414.

Satish-Kumar, M., So, H., Yoshino, M., Kato, M., Hiroi, Y., 2011. Experimental determination of carbon isotope fractionation between iron carbide melt and carbon: ^{12}C -enriched carbon in Earth's core? *Earth Planet. Sci. Lett.* 310, 340–348.

Sedwick, P.N., McMurtry, G.M., Hilton, D.R., Goff, F., 1994. Carbon dioxide and helium in hydrothermal fluids from Loihi Seamount, Hawaii, USA: temporal variability and implications for the release of mantle volatiles. *Geochim. Cosmochim. Acta* 58, 1219–1227.

Shilobreeva, S., Martinez, I., Busigny, V., Agrinier, P., Laverne, C., 2011. Insights into C and H storage in the altered oceanic crust: results from ODP/IODP Hole 1256D. *Geochim. Cosmochim. Acta* 75, 2237–2255.

Shirey, S.B., Smit, K.V., Pearson, D.G., Walter, M.J., Aulbach, S., Brenker, F.E., Bureau, H., Burnham, A.D., Cartigny, P., Chacko, T., Frost, D.J., Hauri, E.H., Jacob, D.E., Jacobsen, S.D., Kohn, S.C., Luth, R.W., Mikhail, S., Navon, O., Nestola, F., Nimis, P., Palot, M., Smith, E.M., Stachel, T., Stagni, V., Steele, A., Stern, R.A., Thomassot, E., Thomson, A.R., Weiss, Y., 2019. Diamonds and the mantle geodynamics of carbon. In: Orcutt, B.N., Daniel, I., Dasgupta, R. (Eds.), *Deep Carbon: Past to Present*. Cambridge Univ. Press, pp. 89–128.

Sobolev, A.V., Hofmann, A.W., Jochum, K.P., Kuzmin, D.V., Stoll, B., 2011. A young source for the Hawaiian plume. *Nature* 576, 434–439.

Sun, W.-d., Hawkesworth, C.J., Yai, C., Zhang, C.-c., Huang, R.-f., Liu, X., Sun, X.-l., Ireland, T., Song, M.-s., Ling, M.-x., Ding, X., Zhang, Z.-f., Fan, W.-m., Wu, Z.-q., 2018. Carbonated mantle domains at the base of the Earth's transition zone. *Chem. Geol.* 478, 69–75.

Trull, T.W., Nadeau, S., Pineau, F., Polv  , M., Javoy, M., 1993. C-He systematics in hotspot xenoliths: implications for mantle carbon contents and carbon recycling. *Earth Planet. Sci. Lett.* 118, 43–64.

Tucker, J.M., Hauri, E.H., Pietruszka, A.J., Garcia, M.O., Marske, J.P., Trusdell, F.A., 2019. A high carbon content of the Hawaiian mantle from olivine-hosted melt inclusions. *Geochim. Cosmochim. Acta* 254, 156–172.

Tucker, J.M., Mukhopadhyay, S., Gonnermann, H.M., 2018. Reconstructing mantle carbon and noble gas contents from degassed mid-ocean ridge basalts. *Earth Planet. Sci. Lett.* 496, 108–119.

Valbracht, P.J., Staudacher, T.J., Malahoff, A., All  re, C.J., 1997. Noble gas systematics of deep rift zone glasses from Loihi Seamount, Hawaii. *Earth Planet. Sci. Lett.* 150, 399–411.

Valbracht, P.J., Staudigel, H., Honda, M., McDougall, I., Davies, G.R., 1996. Isotopic tracing of volcanic source regions from Hawaii: decoupling of gaseous from lithophile magma compositions. *Earth Planet. Sci. Lett.* 144, 185–198.

White, W.M., 1985. Sources of oceanic basalts: radiogenic isotopic evidence. *Geology* 13, 115–118.

Wilding, J.D., Zhu, W., Ross, Z.E., Jackson, J.M., 2023. The magmatic web beneath Hawai'i. *Science* 379, 462–468. <https://doi.org/10.1126/science.ade5755>.

Williams, C.D., Li, M., McNamara, A.K., Garnero, E.J., van Soest, M., 2015. Episodic entrainment of deep primordial mantle material into ocean island basalts. *Nat. Commun.* <https://doi.org/10.1038/ncomms9937>.

Williams, C.D., Mukhopadhyay, S., Rudolph, M.L., Romanowicz, B., 2019. Primitive helium is sourced from seismically slow regions in the lowermost mantle. *Geochim. Geophys. Geosyst.* 20, 4130–4145.

Zhang, X.-Y., Chen, L.-H., Wang, X.-J., Hanyu, T., Hofmann, A.W., Komiya, T., Nakamura, K., Kato, Y., Zeng, G., Gou, W.-X., Li, W.-Q., 2022. Zinc isotopic evidence for recycled carbonate in the deep mantle. *Nat. Commun.* 13.